Infrared-Based Measurements of Velocity, Turbulent Kinetic Energy, and Dissipation at the Water Surface in a Tidal River

C. Chris Chickadel, Stefan A. Talke, Alexander R. Horner-Devine, and Andrew T. Jessup, *Member, IEEE*

***Abstract*—Thermal infrared (IR)-based particle image velocimetry (PIV) is used to measure the evolution of velocity, turbulent kinetic energy (TKE), and the TKE dissipation rate at the water surface in the tidally influenced Snohomish River. Patterns of temperature variability in the IR imagery arise from disruption of the cool-skin layer and are used to estimate the 2-D velocity field. Comparisons of IR-based PIV mean velocity made with a colocated acoustic velocimeter demonstrate high correlation ($r^2 > 0.9$). Over a tidal period, surface TKE computed from the IR velocity varies from 10^{-4} to 3×10^{-3} J $\cdot$ kg^{-1}, with an average difference from the *in situ* measurements of 8%. IR-derived TKE dissipation rates vary from approximately 3×10^{-6} to 2×10^{-4} W $\cdot$ kg^{-1} at peak ebb, agreeing on average to within 7% of the *in situ* velocimeter results. IR-based PIV provides detailed measurements of previously inaccessible surface velocities and turbulence statistics.**

***Index Terms*—Flow, image motion analysis, infrared (IR) imaging, rivers, turbulence, velocity field.**

I. Introduction

TURBULENCE in rivers and estuaries affects water quality, ecosystem processes, and channel morphology by redistributing and mixing momentum, nutrients, pollutants, heat, and salinity. On a large scale, the production of turbulent kinetic energy (TKE) and its dissipation control the evolution of tides and the density structure of estuaries [1], [2]. At the water surface (air–water interface), the dissipation of TKE in the water controls the exchange of gas between water and air [3] and hence determines the re-aeration of oxygen-depleted waters and the exchange of carbon dioxide.

Despite the importance of mixing and transport in rivers and estuaries, *in situ* measurements of turbulence using current meters, scalar tracers, and other techniques are challenging to make accurately, often distort the flow field, and typically lack the spatial resolution needed to assess complex flow patterns. Here, we present novel remote measurements of flow and turbulence using 2-D thermal infrared (IR) imaging of the water surface. The technique is predicated on the observation that turbulence and coherent structures (e.g., boils and vortices) generate multiscale temperature variability on the water surface through the disruption of an $O(1$ mm$)$ thick cool-skin layer that is formed by net heat loss to the atmosphere at the water surface [4], which is a common occurrence for low wind speeds and in the absence of strong solar heating. The surface temperature variability is then advected and distorted by surface currents (see supplemental video). We exploit these shifting surface temperature patterns to measure flow velocity, TKE, and TKE dissipation rate (ε) using particle image velocimetry (PIV), which is a technique used extensively in laboratory experiments, e.g., [5], because it is noninvasive and provides greater spatial resolution than *in situ* current meters.

We investigate the dynamics of turbulence right at the water surface, a region that is difficult to measure in the field and yet is critical to air–water heat and gas transfer. PIV techniques have been applied using thermal imagery in laboratory experiments [6], [7] and in the open ocean [8]. To our knowledge, this is the first study to validate the thermal PIV results with *in situ* measurements. Unlike previous studies, which describe wave-breaking processes in the laboratory or ocean, we focus on the surface expression of open channel flow and turbulence characteristics generated from below. Hence, we demonstrate the surprising result that surface flow can be considered isotropic at scales below $O(1$ m$)$, which permits the use of the inertial cascade method in estimating the TKE dissipation rate.

II. Measurements

Centimeter-resolution IR measurements of the river surface temperature field and colocated subsurface velocity were recorded during a two-week experiment on the Snohomish River in Washington State during September 2009. The study site, which is 15 km upstream of the river mouth at Puget Sound, has a tidal range of 3 m and a maximum tidal velocity of 0.8 m s^{-1}. Salinity intrusion was only occasionally detected during spring tides and was not present during the set of measurements considered here. Measurements were made from the *R/V Henderson*, which is a 65-ft twin-hulled powered research barge held stationary in the river flow by two

Manuscript received October 14, 2010; revised January 20, 2011; accepted March 1, 2011. Date of publication April 21, 2011; date of current version August 26, 2011. This work was supported by the Department of Defense and Office of Naval Research Multidisciplinary University Research Initiative under Grant N00014-05-1-0485. This paper has supplementary downloadable material available at http://ieeexplore.ieee.org, provided by the authors. This includes one multimedia MP4 format movie clip, which shows a PIV boil flow example: thermal infrared video and PIV velocity anomaly of passing river boils. This material is 7.26 MB in size.

C. C. Chickadel and A. T. Jessup are with the Applied Physics Laboratory, University of Washington, Seattle, WA 98105 USA (e-mail: chickadel@apl.uw.edu; jessup@apl.uw.edu).

S. A. Talke was with the Civil and Environmental Engineering Department, University of Washington, Seattle, WA 98195 USA. He is now with the Civil and Environmental Engineering Department, Portland State University, Portland, OR 97207 USA (e-mail: stefant@cecs.pdx.edu).

A. R. Horner-Devine is with the Civil and Environmental Engineering Department, University of Washington, Seattle, WA 98195 USA (e-mail: arhd@uw.edu).

Digital Object Identifier 10.1109/LGRS.2011.2125942

1545-598X/$26.00 © 2011 IEEE

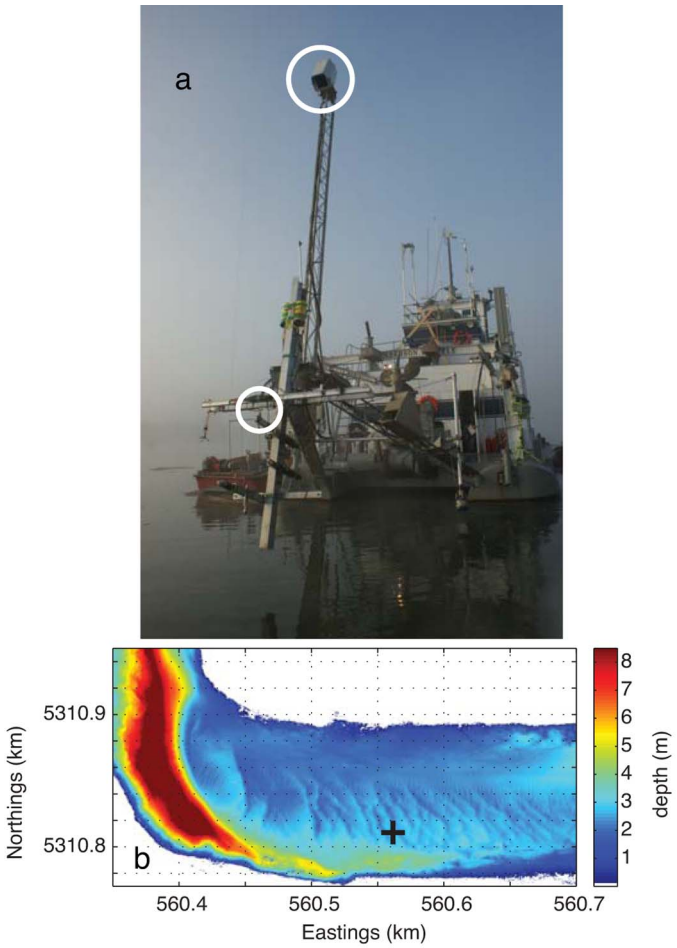

Fig. 1. (a) Photograph of the IR camera and ADV array on the barge instrument frame prior to deployment (the upper and lower white circles highlight the aerial IR camera and near-surface ADV, respectively). (b) Multibeam bathymetry of the Snohomish River and $(+)$ location of the barge sampling location analyzed here. River flow during ebb tide is from east to west (right to left in the plot).

retractable pilings (or spuds). During a tidal cycle, the barge floated freely up and down the spuds, with no flow-induced swinging or rocking of the barge motion except during large boat wakes. An array of acoustic Doppler velocimeters (ADVs) was positioned at the end of an 8-m instrument frame on the upstream end of the vessel [Fig. 1(a)]. An Indigo Phoenix 640 $\times$ 512 QWIP array camera (8–9.2-μm spectral response and 25-mK noise-equivalent temperature difference) was affixed in a down-looking position (13.9° incidence) atop a 6-m tower on the end of the frame, such that the field of view included the surface locations of the ADV measurements.

Here, we analyze an ebb tide during the night of September 24, 2009, when atmospheric conditions were calm and clear and there was no density stratification. The river bottom at the study site was characterized by large dunes with an average wavelength of 10 m and a height of 0.5 m [Fig. 1(b)] in water depth that decreased from 5.5 to 2.5 m over the course of the ebb tide. The barge was positioned with the instrument frame upstream of the hull, and measurements were made during the night to maximize the temperature contrast between water and the atmosphere and to avoid waves that occur due to daytime winds and boat traffic.

A. IR-Based Surface Velocimetry

A PIV analysis was performed on the IR image data collected at a frequency of 5 Hz (subsampled from 20-Hz data) with a 4.5 m $\times$ 3.5 m field of view. The average pixel resolution over the imaged field is 7.5 mm, providing resolution of fine-scale temperature features. The camera was periodically corrected for image nonuniformity and spatial noise via a two-point blackbody calibration.

The PIV technique measures horizontal velocity by tracking shifts in coherent temperature patterns across sequences of IR images. Typical PIV uses normalized cross-correlation between image pairs [5], but the technique used here is based on phase correlation to better define image feature motion in the presence of large-scale background variation [9]. The basic algorithm assumes some small uniform shift (x_0, y_0) in pairs of images I_1 and I_2

$$I_2(x, y) = I_1(x - x_0, y - y_0). \tag{1}$$

The cross-stream and along-stream directions are x and y, respectively. The corresponding phase correlation map between I_1 and I_2 is estimated as

$$P(x, y) = \mathcal{F}^{-1}\left(\frac{\hat{I}_1^* \hat{I}_2}{\left|\hat{I}_1^* \hat{I}_2\right|} G\right) \tag{2}$$

where $\mathcal{F}^{-1}$ is the inverse 2-D Fourier transform operator, $\hat{()}$ indicates the Fourier transformed image, $(^*)$ is the complex conjugate, and G is a Gaussian-shaped window with unit peak amplitude centered at the origin and a width (equivalent to twice the standard deviation) of two-thirds of the analysis window size. For a set of continuous and infinite length images, the raw phase map is analytically represented as a delta (impulse) function centered at (x_0, y_0) [10], and the feature shift is found by locating this peak. The multiplication of G in the frequency domain results in a Gaussian-shaped phase correlation peak in the spatial domain using the convolution theorem. However, fidelity of the velocity estimation is limited to unit pixel shifts if the discrete phase correlation maximum is used. Therefore, we obtain subpixel refinement by using the calculated peak location of a 2-D Gaussian hump fit to the phase correlation map within a three-point radius of the discrete peak, e.g., [11]. The full PIV algorithm uses a multipass implementation of the aforementioned basic method with decreasing interrogation window sizes, so that subsequent PIV velocity estimates are refinements of prior estimates, thus enabling better estimation in regions of high-velocity gradients. In this processing, we have used interrogation windows with 50% overlap, starting with 450 $\times$ 450 pixels, continuing with 128 $\times$ 128 and 32 $\times$ 32 pixels, and culminating with a 16 $\times$ 16 pixel window for a final velocity field with 6-cm spatial resolution (Fig. 2). The PIV algorithm was applied to sequential images to produce 5-Hz time series of the 2-D velocity field (see the supplementary video).

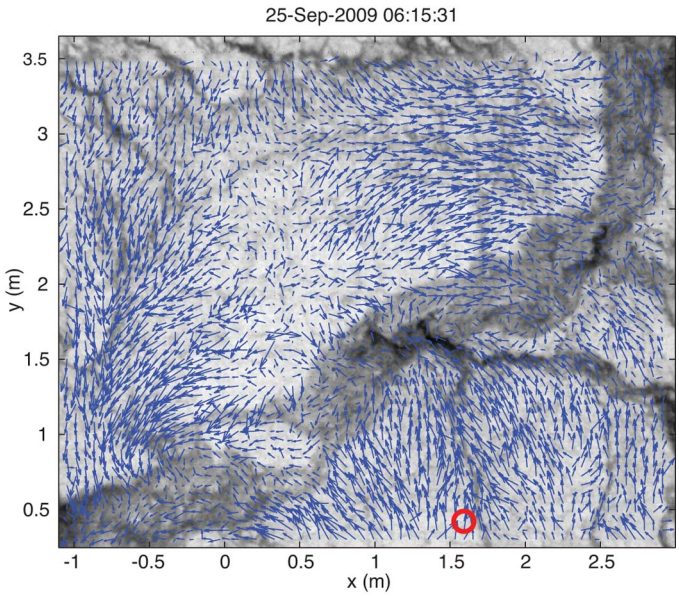

Fig. 2. Example of the convergence between two river boils in an IR image and the associated vector field of the turbulent (mean-removed) velocity derived from PIV. The brighter regions in the underlying IR image are warmer, and (white to black) the displayed temperature range is less than 0.7° K. (Arrow length) The maximum velocity magnitude shown is 11 cm $\cdot$ s^{-1}, and the circle indicates the location of the near-surface ADV and PIV analysis location used for comparison. Time is in Coordinated Universal Time.

B. *In Situ* Flow Measurements

The array of ADVs was mounted on the barge, with sampling depths of 1.5, 0.7, 0.4, and 0.02 m below the surface [Fig. 1(a)]. To avoid influence from the boat hull and to be colocated within the IR field of view, these instruments were mounted on a rigid aluminum frame attached to a cantilevered A-frame, both of which were further stiffened with multiple cable stays. The instruments were aligned with the axis of the barge, and the alignment was verified after the experiment with surveys using an optical total station. Visual assessment of the *in situ* velocities confirms that surface waves (which can contaminate turbulence estimates) were negligible during the experiment.

To provide the best comparison with surface PIV flow estimates, we focus on measurements with an upward-facing ADV whose sample volume was located 2 cm below the water surface [Fig. 1(a)]. The ADV sampled continuously at 25 Hz and was subsampled to 5 Hz for comparison with the PIV sampling rate. We corrected for a rotational offset of 13 ° between the PIV and ADV measurements. The ADV measurement is located within 3 cm of the nearest PIV velocity estimate used for comparison (Fig. 2).

III. Results

The IR image data reveal a rich pattern of temperature contrast on the river surface. Boils at the surface produce areas of warmer (brighter) upwelled water contrasted against regions in which the cool-skin layer remains undisturbed (Fig. 2; supplemental video). These features advect downstream with the mean flow and evolve, as documented by the pattern of mean-removed (turbulent) velocity. The observed turbulent velocity field in Fig. 2 consists of divergent upwelling flow in the

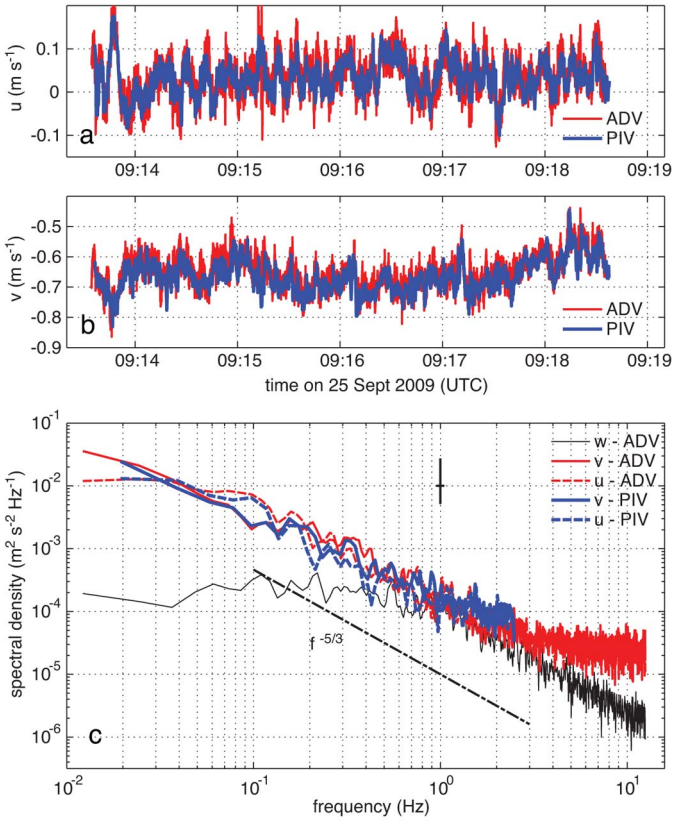

Fig. 3. Example of a 5-min ADV and IR-based PIV time series of the (a) lateral u and (b) along-stream ν components of flow (negative is downstream flow). ADV and PIV velocities were sampled at 25 and 5 Hz, respectively. (c) Spectra from the measured u, ν, and w (vertical velocity) components using ADV and IR PIV, with a 95% confidence limit and an $f^{5/3}$ slope indicated. The spectra show good agreement over the majority of the frequency range, and both methods show a noise floor at $f > 1.5$ Hz in the horizontal components. ADV-measured w contains less energy at low frequencies compared with u and ν, consistent with confinement due to the free surface.

center of an active boil ($x = 0.2$ m and $y = 2.2$ m). This flow converges with the upstream edge of a second boil located downstream (lower right corner), in which fluid is slower than the mean and hence appears to be directed upstream. The large center convergence (downwelling) area appears as a cooler temperature.

The 2-D velocity fields (Fig. 2) are validated by comparing the subsurface ADV velocity with the nearest velocity estimate on the PIV grid. The 3-min mean along-stream flow and cross-stream flow ($\langle\nu\rangle$ and $\langle u\rangle$) and its temporal perturbation (ν' and u') estimated with the PIV technique agree well with the *in situ* velocimeter measurements [Fig. 3(a) and (b)]. Similarly, the power spectra [Fig. 3(c)] of cross-stream and along-stream velocities derived from PIV and from the *in situ* velocimeter are in agreement, particularly for larger scale motions with a frequency (f) of less than 1 Hz. For $f > 2$ Hz, the horizontal spectra begin leveling out, indicating that a noise floor is approached. The spectra from both instruments exhibit an $f^{-5/3}$ decay, which is consistent with a turbulent cascade transferring energy from large to small scales [12]. We use this observation later to estimate turbulent energy dissipation, as also done, for example, in [13] for surface measurements in

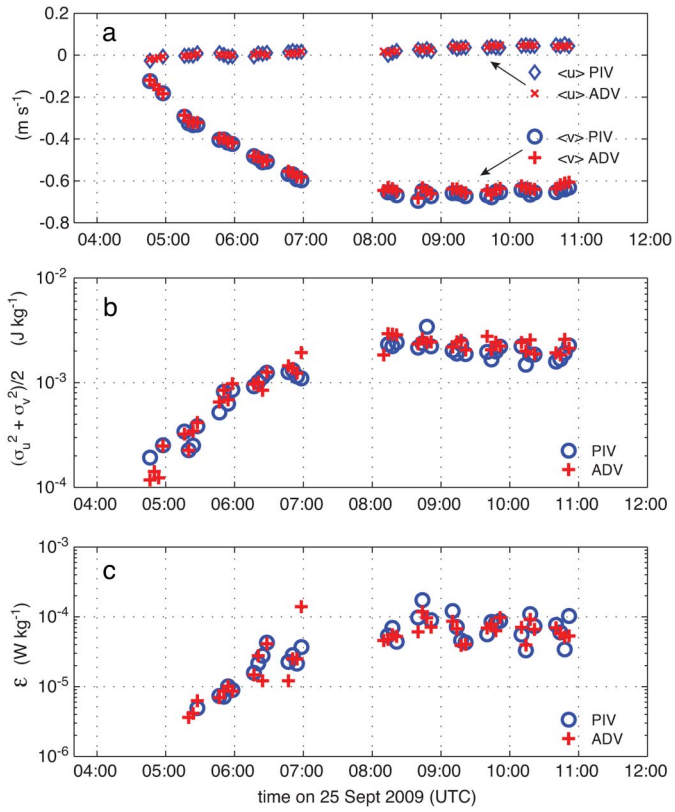

Fig. 4. Time series comparisons of 3-min statistics over an ebb tide, including (a) mean along-stream ($\langle\nu\rangle$) and cross-stream ($\langle u\rangle$) velocities, (b) computed horizontal TKE, and (c) computed turbulent energy dissipation rate (ε).

a laboratory. Over a tidal period, 3-min averaged along-stream velocities ($\langle\nu\rangle$) are highly correlated with ADV measurements [$r^2 = 0.99$; Fig. 4(a)]. Cross-stream mean velocities ($\langle u\rangle$) are similarly correlated ($r^2 = 0.94$). The combined PIV velocity components (magnitudes) are approximately 2% larger than ADV estimates.

The correlation between the fluctuating components of the PIV and ADV velocity measurements suggests that IR PIV can be used to estimate TKE. We note that vertical fluctuations are suppressed by the surface boundary condition at the energy-containing low-frequency scales [see Fig. 3(c)]; hence, the total TKE is dominated by along- and cross-stream velocity variances. The 3-min along- and cross-stream components of TKE, $\langle\nu'^2\rangle/2$ and $\langle u'^2\rangle/2$, respectively, from the surface PIV measurement compare well with the *in situ* measurement [Fig. 4(b)]. As the flow accelerates during the ebb, surface TKE increases from 10^{-4} J $\cdot$ kg^{-1} to a peak of 3×10^{-3} J $\cdot$ kg^{-1}. PIV and ADV TKE estimates are well correlated ($r^2 = 0.85$), although PIV-derived TKE is, on average, $\sim$8% lower than the *in situ* estimate.

The presence of a $-5/3$ slope in the log–log power spectra suggests that ε can be estimated using the inertial subrange of the ν' wavenumber spectra [12]. Assuming that turbulence at small scales is statistically isotropic (an assumption in [14]), we use the Taylor frozen turbulence hypothesis to estimate the wavenumber k and the wavenumber spectra by $k = 2\pi f/\langle\nu\rangle$ and $\tilde{\phi}(k) = S(f) \cdot \langle\nu\rangle/(2\pi)$, respectively, where $S(f)$ is the power spectrum of $\nu'(t)$. These wavenumber spectra estimates are fitted to the expected turbulence cascade model

$$\phi(k) = \alpha\varepsilon^{\frac{2}{3}}k^{-\frac{5}{3}} \tag{3}$$

over the range $0.25 < k < 3.3$, where the constant α is taken as 0.5 [12]. We eliminate ε estimates when the fit to $\phi(k)$ results in log–log wavenumber slopes in the inertial subrange of less than -2 or greater than $-3/4$.

As the tidal flow accelerates, the resulting near-surface dissipation rates vary by roughly two orders of magnitude from less than 3×10^{-6} W $\cdot$ kg^{-1} right after slack water to nearly 2×10^{-4} W $\cdot$ kg^{-1} during peak ebb [Fig. 4(c)]. The IR-based PIV measurements of ε reproduce the tidal trends in the ADV data ($r^2 = 0.59$), with PIV dissipation rates approximately 7% higher than *in situ* estimates, on average. We attribute the small difference in TKE and ε between methods to the larger noise of the PIV estimates compared to ADV measurements, the spatial resolution of the PIV, and possible flow bias from the *in situ* measurement frame.

IV. Discussion and Summary

The surface velocity measured with the IR PIV technique closely matches the near-surface flow pattern measured *in situ*, validating our approach and providing a method for new insights into the surface expression of coherent structures and turbulence. The well-resolved turbulent velocity signal allows for the calculation of higher order statistics such as TKE and ε. These statistics match the tidal progression of TKE and ε measured by an *in situ* ADV during all periods observed. We note, however, that the apparent increased noise of IR-based PIV will limit estimates of ε to times when the TKE is sufficient to overcome measurement noise. Furthermore, the IR PIV technique relies on sufficient temperature contrast to resolve surface motion, which is almost always present due to surface heating or cool-skin formation. Future improvement should focus on refined PIV algorithms and increasing the spatial resolution of the IR imager to decrease noise.

The presence of a $-5/3$ slope in the velocity spectra at the water surface is a surprising result, since Kolmogorov [14] assumes that an inertial cascade requires isotropic conditions. Because vertical velocity fluctuations are suppressed by the surface (kinematic) boundary condition, the surface flow is highly anisotropic and is not expected to have a turbulent cascade. However, other studies have also found a $-5/3$ slope at the surface, e.g., [15], and used the inertial subrange method to estimate the dissipation rate, noting however that its interpretation is a topic under debate [16].

We investigate this conundrum by examining the near-surface anisotropy at different scales. At large scales (low frequency), the ratio of vertical to horizontal fluctuations measured 2 cm below the water surface is quite small (Fig. 5); hence, large-scale flow variations are anisotropic. However, this ratio approaches near unity at $f = 1$ Hz or $k = 1.5$ m^{-1} (at maximum flow), so that fluctuations with a frequency $\geq$1 Hz can be considered to be isotropic. Interestingly, the $-5/3$ slope occurs between 1 and 12.5 Hz (the Nyquist frequency) in the

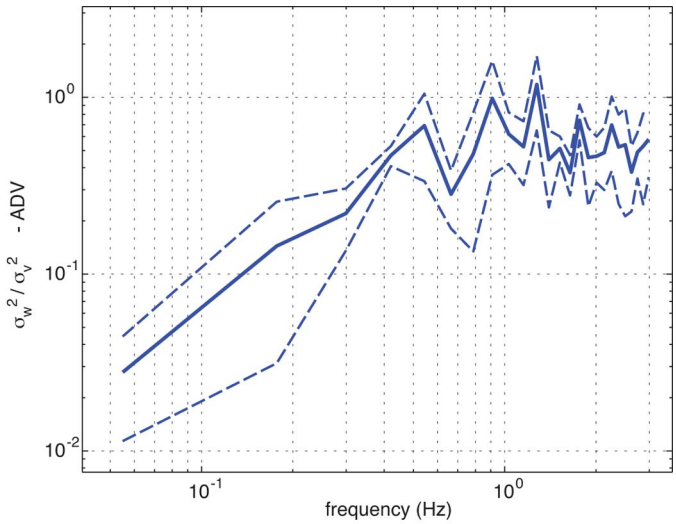

Fig. 5. Frequency dependence of anisotropy based on the ratio of vertical to horizontal variances in the turbulent velocity fluctuations in ADV measurements, using spectra from Fig. 3(c). (Solid line) Mean (dashed lines) plus or minus one standard deviation anisotropy values were calculated over 0.12-Hz width bins. Only values outside of the noise floor ($frequency < 1.5$ Hz) are shown.

w' spectra, but it only occurs between roughly 0.1 and 2 Hz for the u' and v' spectra (Fig. 3). The lack of a $-5/3$ cascade for the horizontal spectra for frequencies above 2 Hz reflects the noise floor of the instruments and is not physical (the vertical resolution of an ADV is approximately four times the horizontal resolution). This noise causes a spurious decrease in the anisotropy ratio between 2 and 12 Hz.

Although the overlap between the range of scales exhibiting the $-5/3$ behavior in the horizontal and vertical components is somewhat limited, both clearly lie along the same line (i.e., have the same slope and intercept). Thus, dissipation rates computed using the lower frequency $-5/3$ range of the spectrum in the horizontal components match the dissipation rates computed from the higher frequency range in the vertical component. It is likely that the observed cascade for the horizontal components is inherited from lower in the water column and is not restricted by the surface boundary condition. In the vertical direction, the surface boundary more severely restricts the larger scales than the small scales [16] and produces the observed roll-off in the power spectrum. The results in Figs. 4 and 5 suggest a less stringent condition for the inertial cascade, namely, that flow must only be isotropic at small scales. In addition, dissipation rates can be estimated from the horizontal velocity components at scales larger than those scales that are blocked in the vertical component.

To our knowledge, these are the first natural turbulence measurements using PIV applied to IR imagery to be validated with colocated *in situ* observations. This result presents an opportunity to remotely sense turbulence exactly at the water surface, through which important fluxes occur. On a fine scale, the intricate pattern of turbulent motions on the surface and their relation to subsurface turbulence profiles and bottom roughness can be explored. An improved understanding of the surface expression of subsurface turbulence may provide new insights into the processes responsible for air–water fluxes of gas and heat in rivers, estuaries, and any environment characterized by full water-column mixing due to flow over bathymetry. On a large scale, application of this technique to larger fields of view could be used to measure spatial variation in flow and turbulent statistics due to a river geometry (e.g., bends) or bottom bathymetry with unprecedented resolution.

ACKNOWLEDGMENT

The authors would like to thank D. Clark, R. Branch, and the students of the UW EFML for their tireless efforts in data collection. They would also like to thank the APL Marine Operations (E. Boget, Head) and the operators and engineers of *R/V Henderson*.

REFERENCES

[1] C. T. Friedrichs and D. G. Aubrey, "Tidal propagation in strongly convergent channels," *J. Geophys. Res.*, vol. 99, no. C2, pp. 3321–3336, Feb. 1994.

[2] P. MacCready, "Towards a unified theory of tidally averaged estuarine salinity structure," *Estuaries*, vol. 27, no. 4, pp. 561–570, Aug. 2004.

[3] C. J. Zappa, W. R. McGillis, P. A. Raymond, J. B. Edson, E. J. Hintsa, H. J. Zemmelink, J. W. H. Dacey, and D. T. Ho, "Environmental turbulent mixing controls on air–water gas exchange in marine and aquatic systems," *Geophys. Res. Lett.*, vol. 34, p. L10 601, 2007.

[4] P. M. Saunders, "The temperature at the ocean–air interface," *J. Atmos. Sci.*, vol. 24, no. 3, pp. 269–273, May 1967.

[5] R. J. Adrian, "Twenty years of particle image velocimetry," *Exp. Fluids*, vol. 39, no. 2, pp. 159–169, Aug. 2005.

[6] C. S. Garbe, H. Spies, and B. Jähne, "Estimation of complex motion from thermographic image sequences," *Proc. SPIE*, vol. 5073, pp. 303–317, 2003.

[7] A. T. Jessup and K. R. Phadnis, "Measurement of the geometric and kinematic properties of microscale breaking waves from infrared imagery using a PIV algorithm," *Meas. Sci. Technol.*, vol. 16, no. 10, pp. 1961–1969, Oct. 2005.

[8] F. Veron, W. K. Melville, and L. Lenain, "Infrared techniques for measuring ocean surface processes," *J. Atmos. Ocean. Technol.*, vol. 25, no. 2, pp. 307–326, Feb. 2008.

[9] M. P. Wernet, "Symmetric phase only filtering: A new paradigm for DPIV data processing," *Meas. Sci. Technol.*, vol. 16, no. 3, pp. 601–618, Mar. 2005.

[10] R. N. Bracewell, *The Fourier Transform and Its Applications*. New York: McGraw-Hill, 1986.

[11] A. C. Eckstein, J. Charonko, and P. Vlachos, "Phase correlation processing for DPIV measurements," *Exp. Fluids*, vol. 45, no. 3, pp. 485–500, Sep. 2008.

[12] H. Tennekes and J. L. Lumley, *A First Course in Turbulence*. Cambridge, MA: MIT Press, 1972.

[13] B. H. Brumley and G. H. Jirka, "Near-surface turbulence in a grid-stirred tank," *J. Fluid Mech.*, vol. 183, pp. 253–263, 1987.

[14] A. N. Kolmogorov, "The local structure of turbulence in incompressible viscous fluid for very large Reynolds number," *Dokl. Akad. Nauk SSSR*, vol. 30, no. 4, pp. 301–305, 1941.

[15] A. Tamburrino and J. S. Gulliver, "Free-surface turbulence measurements in an open channel flow," in *ASME, FED*, vol. 181, E. P. Rood and J. Katz, Eds. New York: ASME, 1994, pp. 103–112.

[16] D. B. Moog and G. H. Jirka, "Air–water gas transfer in uniform channel flow," *J. Hydraul. Eng.*, vol. 125, no. 1, pp. 3–10, Jan. 1999.